

## Sputtering and heating of Titan's upper atmosphere

BY ROBERT E. JOHNSON<sup>1,2,\*</sup>

<sup>1</sup>*University of Virginia, Charlottesville, VA 22904, USA*

<sup>2</sup>*Department of Physics, New York University, New York, NY 10003, USA*

Titan is an important endpoint for understanding atmospheric evolution. Prior to Cassini's arrival at Saturn, modelling based on Voyager data indicated that the hydrogen escape rate was large ( $1\text{--}3 \times 10^{28}$  amu s<sup>-1</sup>), but the escape rates for carbon and nitrogen species were relatively small ( $5 \times 10^{26}$  amu s<sup>-1</sup>) and dominated by atmospheric sputtering. Recent analysis of the structure of Titan's thermosphere and corona attained from the Ion and Neutral Mass Spectrometer and the Huygens Atmospheric Structure Instrument on Cassini have led to substantially larger estimates of the loss rate for heavy species ( $0.3\text{--}5 \times 10^{28}$  amu s<sup>-1</sup>). At the largest rate suggested, a mass that is a significant fraction of the present atmosphere would have been lost to space in 4 Gyr; hence, understanding the nature of the processes driving escape is critical. The recent estimates of neutral escape are reviewed here, with particular emphasis on plasma-induced sputtering and heating. Whereas the loss of hydrogen is clearly indicated by the altitude dependence of the H<sub>2</sub> density, three different one-dimensional models were used to estimate the heavy-molecule loss rate using the Cassini data for atmospheric density versus altitude. The solar heating rate and the nitrogen density profile versus altitude were used in a fluid dynamic model to extract an average net upward flux below the exobase; the diffusion of methane through nitrogen was described below the exobase using a model that allowed for outward flow; and the coronal structure above the exobase was simulated by presuming that the observed atmospheric structure was due to solar- and plasma-induced hot particle production. In the latter, it was hypothesized that hot recoils from photochemistry or plasma-ion-induced heating were required. In the other two models, the upward flow extracted is driven by heat conduction from below, which is assumed to continue to act above the nominal exobase, producing a process referred to as 'slow hydrodynamic' escape. These models and the resulting loss rates are reviewed and compared. It is pointed out that preliminary estimates of the composition of the magnetospheric plasma at Titan's orbit appear to be inconsistent with the largest loss rates suggested for the heavy species, and the mean upward flow extracted in the one-dimensional models could be consistent with atmospheric loss by other mechanisms or with transport to other regions of Titan's atmosphere.

**Keywords:** Titan; Saturn; atmosphere; escape; sputtering; evolution

---

\*Address for correspondence: University of Virginia, Thornton Hall B102, PO Box 400238, Charlottesville, VA 22904, USA (rej@virginia.edu).

One contribution of 14 to a Discussion Meeting Issue 'Progress in understanding Titan's atmosphere and space environment'.

## 1. Introduction

Titan is unique among the outer Solar System satellites in that it has an atmosphere with a column density about 10 times that of the Earth and an atmospheric mass to solid mass ratio comparable to that of Venus. If Io, Europa or Ganymede had a large Titan-like atmosphere in some earlier epoch, it would have been removed by the plasma trapped in the Jovian magnetosphere even at present Jovian plasma densities (Johnson 2004). Therefore, the use of Cassini spacecraft data to determine the heating and the present erosion rate of Titan's atmosphere by the plasma trapped in Saturn's magnetosphere will provide a useful endpoint for understanding the plasma-induced erosion and heating of other planetary and satellite atmospheres.

Although Titan's atmosphere has about 10 times the column density of the Earth's atmosphere, the measured  $^{15}\text{N}/^{14}\text{N}$  ratio suggests that considerable escape has occurred (Niemann *et al.* 2005; Waite *et al.* 2005). A number of active escape processes have been proposed: thermal escape (Cui *et al.* 2008); chemical-induced escape (De La Haye *et al.* 2007*b*); slow hydrodynamic escape (Strobel 2008; Yelle *et al.* 2008); pick-up ion loss and ionospheric outflow (Ledvina *et al.* 2005; Wahlund *et al.* 2005; Ma *et al.* 2006; Sillanpaa *et al.* 2006; Coates *et al.* 2007); and plasma-induced atmospheric sputtering (Shematovich *et al.* 2003; Michael *et al.* 2005*a*; De La Haye *et al.* 2007*a*). In addition, atmosphere is lost by methane destruction and hydrocarbon precipitation to the surface. These processes are briefly reviewed below, with special emphasis on the role of the magnetospheric and ionospheric plasma flowing through the exobase regions. The role of the plasma in Titan's thermosphere and corona is interesting in that it can vary considerably depending on whether Titan is in Saturn's magnetosphere exposed to the trapped magnetospheric plasma or outside the boundary and exposed to the solar wind flux (Penz *et al.* 2005). It can also vary due to the highly variable ambient plasma pressure, which occurs for a number of reasons (Ma *et al.* 2006; Sillanpaa *et al.* 2006), including Titan passing in to and out of the current sheet.

Direct simulation Monte Carlo (DSMC) models have been used to calculate the plasma-induced heating and loss at Titan (Shematovich *et al.* 2003; Michael & Johnson 2005; Michael *et al.* 2005*a*), referred to as atmospheric sputtering. Such simulations were also used to calibrate useful analytic models of atmospheric sputtering (Johnson 1994; Johnson *et al.* 2000). These results were subsequently used in preliminary interpretations of Cassini Ion and Neutral Mass Spectrometer (INMS) data in Titan's exobase region (De La Haye *et al.* 2007*a*). In that work, the heating of the thermosphere and corona due to the globally averaged flux of magnetospheric and pick-up ions was compared with the effect of solar UV in the exobase region. Below, we first review aspects of exobase approximation and the recoil spectra used in De La Haye *et al.* (2007*a*). The results from that paper are then compared with more recent descriptions of escape based on much different interpretations of the Cassini INMS data (Cui *et al.* 2008; Strobel 2008; Yelle *et al.* 2008).

## 2. Exobase and escape depth

Since a planet's atmosphere decreases in density with increasing distance from its centre, an altitude is eventually reached above which molecules can travel planetary-scale distances with a very small probability of making a collision.

At such altitudes an atom or molecule can escape to space if its radial velocity is outward and its energy is greater than its gravitational binding energy. This region of the atmosphere is called the exosphere or the planetary corona. The lower boundary for this region, called the exobase, is defined as that altitude where the ratio of the mean free path for collisions,  $\lambda_c$ , to the atmospheric scale height,  $H$ , is about unity. In rarefied gas dynamics this ratio is the Knudsen number:  $Kn = \text{mean free path} / \text{density scale}$ . It defines the transition region from a gas that is dominated by collisions,  $Kn \ll 1$ , and behaves like a fluid, to a gas that should be modelled stochastically,  $Kn \geq 0.1$ . The nominal exobase is  $Kn = \lambda_c / H \sim 1$  (e.g. Johnson *et al.* 2008). Because the exobase level is determined by the collision cross-section, it is different for each species. Unfortunately, in estimating the mean free path, the total collision cross-section is often used and is modelled by a hard-sphere interaction. Since elastic collision cross-sections for hot recoils are typically forward scattering, simulations have shown that the appropriate  $\lambda_c$  is the mean free path prior to a significant momentum transfer collision (e.g. Johnson 1994). Using realistic potentials, such simulations also show that a hot particle of energy  $E$  moving through a background of identical atoms or molecules loses most of its energy in an average distance  $\lambda_c \sim (bn\sigma_d)^{-1}$ , where  $\sigma_d$  is the momentum transfer (diffusion) cross-section of the escaping particle averaged over the composition of the background gas. Here  $b$  is a number that depends slowly on the interaction potential between the escaping molecule and the ambient gas: for a hard-sphere interaction  $b = 2^{1/2}$  (e.g. Strobel 2002); for a steeply varying potential with forward scattering,  $b \sim 0.5$  (Johnson 1990, 1994; Johnson *et al.* 2000).

Because hot atoms and molecules escape from depths well below the nominal exobase, as seen in figure 1, the often-used Chamberlain model (e.g. Chamberlain & Hunten 1987), in which escape occurs from the exobase, gives a rough approximation to atmospheric loss. Assuming hot particles move upwards at random angles, the probability of escape from a radial depth  $r$  in Titan's atmosphere is

$$P_{\text{es}}(r) \approx \exp\left(-\int_r^\infty ds/\lambda_c\right),$$

where  $ds$  is along the particle's path. This is more commonly written for a one-dimensional flat atmosphere as

$$P_{\text{es}}(z, \theta) \approx \exp\left[-\int_z^\infty dz'/(\lambda_c \cos \theta)\right],$$

where  $\theta$  is the direction of motion, assumed upwards, and  $z$  is the altitude above the surface. Since the density of the exosphere is not necessarily exponential, it is better to write:

$$P_{\text{es}}(z, \theta) \approx \exp[-bN(z)\sigma_d/\cos \theta],$$

where  $N(z)$  is the vertical column density above altitude  $z$  in a flat atmosphere [ $N(z) = \int_z^\infty n dz$ ]. Using this expression and isotropic ejection, the average column depth for escape is

$$\overline{N}_{\text{es}} \approx \left[ \int_0^\infty dN \int_0^1 d \cos \theta NP_{\text{es}} \right] / \left[ \int_0^\infty dN \int_0^1 d \cos \theta P_{\text{es}} \right] \approx (2/3b)\sigma_d^{-1}.$$

Therefore, the altitude of the exobase,  $z_x$ , is determined from  $N(z_x) \approx \overline{N}_{\text{es}}$  (e.g. Johnson *et al.* 2000, 2008).

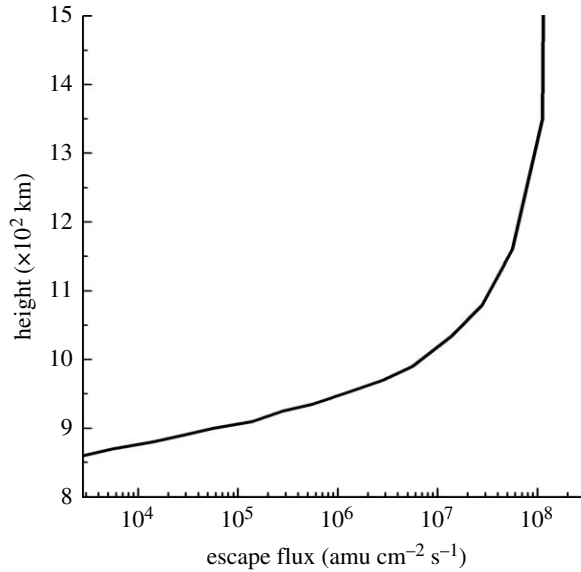


Figure 1. Mass flux for molecular escape versus altitude due to hot atoms produced by photochemistry in Titan's upper atmosphere. From [Shematovich \*et al.\* \(2003\)](#). Exobase ( $Kn \sim 1$ ) is approximately 1500 km in this model. Recoils produced by plasma-induced sputtering have similar loss rates. Although the escape rates differ from those based on recent analysis of INMS data, this figure indicates the depth of origin of escaping molecules: the transition region where the fluid approximation gives way to the kinetic regime.

Simulations and transport equations using realistic potentials give mean escape depths of  $(\overline{N_{\text{es}}}\sigma_{\text{d}}) \sim 1.3$  in a single-component atmosphere (appendix A in [Johnson 1994](#)). Since  $\sigma_{\text{d}}$  decreases slowly with increasing energy and collisions are predominantly forward scattering, evaluating  $\sigma_{\text{d}}$  at the escape energy underestimates  $\overline{N_{\text{es}}}$ . In addition,  $\overline{N_{\text{es}}}$  should be averaged over the hot particle energy distribution, and the integrals above should take into account the fact that Titan's corona is molecular and its composition changes with altitude. In a multicomponent atmosphere similar to Titan's, each species has its own exobase level. Therefore, the exobase for methane is slightly higher than that for nitrogen. These expressions can also be applied to the ions escaping from Titan's ionosphere, but, because their paths are also affected by the local electric and magnetic fields, the integrations above need to be carried out over the ion's path. Since the ion-neutral momentum transfer cross-section,  $\sigma_{\text{d}}$ , is about an order of magnitude larger than the neutral-neutral cross-sections, and is often dominated by the charge exchange, the effect of the ambient plasma on Titan's atmosphere extends well above the nominal exobase for escaping neutrals.

### 3. Hot recoil production

The slowed and deflected ions from the ambient plasma and locally produced pick-up ions can penetrate Titan's atmosphere, transferring momentum to atmospheric neutrals (e.g. [Johnson 1994](#)). This can heat Titan's thermosphere

and produce recoils with sufficient energies to cause escape, processes often referred to as atmospheric sputtering. Atoms and molecules with energies in the eV to few eV range produced by photon- and electron-induced exothermic chemistry also produce recoils that heat the atmosphere and produce escape. However, it has been shown that recoils produced by exothermic chemistry and the incident plasma can be treated together (Johnson 1994; Johnson *et al.* 2000).

The evolution of the initially energized atoms and molecules and their recoils can be described by a Boltzmann transport equation for each molecular species or by the Monte Carlo simulations described below. Because solving the full set of Boltzmann equations is difficult, simplifications are used, such as the exobase approximation described above, the two-stream model (Nagy & Cravens 1981) and the, so-called, 13 moment equations (Hirschfelder *et al.* 1964; Schunk & Nagy 2000). A useful analytical approximation for the energy spectrum of the recoils has been derived from the Boltzmann equation by ignoring spatial and temporal variations in the atmosphere. This has been used extensively in the literature for sputtering of solids and has been applied occasionally for atmospheric sputtering (e.g. Johnson & Luhmann 1998; Johnson *et al.* 2000). A solution to a transport equation in a single-component atmosphere gives the number of hot recoils with energy between  $E$  and  $E+dE$  produced by a primary particle of energy  $E_0$ :  $\eta(E_0, E) dE \approx \beta(E_0/E^{2+x}) dE$  (Johnson 1990, 1994). This result applies for  $E \gg kT$ , where  $T$  is the atmospheric temperature, and  $\beta$  and  $x$  vary slowly with the form for the interaction potential between a hot recoil and an atmospheric molecule. For a steeply varying potential,  $\beta \approx 6/\pi^2$  and  $x \approx 0$  have been shown to be realistic (Sigmund 1981; Johnson 1994). In steady state, the number of moving atoms with energy between  $E$  and  $E+dE$  produced by a source rate  $\phi(t)$  of hot particles of energy  $E_0$  can be written as

$$[\phi(t)/\nu(E)][\delta(E_0 - E) + \eta(E_0, E)]dE.$$

Here the delta function,  $\delta(E_0 - E)$ , accounts for the initial recoil and  $\nu(E)$  is the collision frequency between a hot molecule and a thermal molecule:  $\nu(E) = [vn\sigma_d(E)]$ , where  $v$  is the relative collision velocity, e.g.  $v = (2E/m)^{1/2}$  with  $m$  the mass of the atmospheric recoil and  $E \gg kT$  (Johnson 1994).

Monte Carlo simulations using realistic potentials have been carried out confirming the analytic expressions discussed above (e.g. Johnson *et al.* 2000). Remarkably, these simple expressions were also confirmed in a simulation of a multi-species molecular atmosphere (Cipriani *et al.* 2007). The spectrum of the hot recoils produced by both dissociative recombination and the incident ion flux exhibited power-law dependence over a broad range of energies. In the discussion of their result, the extracted powers were incorrectly compared with the dependence on  $E$  for the total number of recoils produced,  $\eta(E_0, E)$ , rather for the steady-state recoil energy spectrum,  $[\sim \phi(t)\eta(E_0, E)/\nu(E)]$  with which they essentially agree. The latter varies more steeply with  $E$  due to the energy dependence of the collision frequency,  $\nu(E) \propto E^{(1/2+q)}$ , where  $q$  is small (e.g. Johnson 1990). Because the analytic model of the recoil spectrum above has been roughly confirmed by detailed DSMC simulations, it was used in the work of De La Haye *et al.* (2007a) to fit Titan's observed coronal densities.

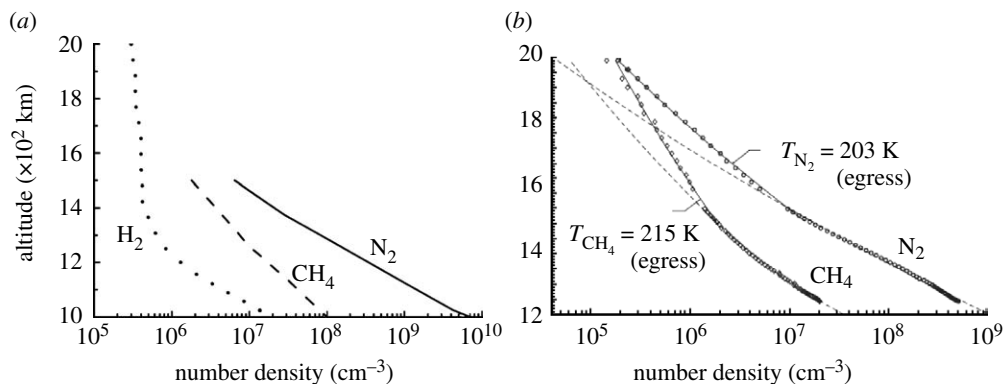


Figure 2. (a) Density profiles for  $\text{H}_2$  based on an *average* of INMS data from Cui *et al.* (2008) and  $\text{N}_2$  and  $\text{CH}_4$  data from Yelle *et al.* (2008). (b) Density versus radial distance from Titan for  $\text{CH}_4$  and  $\text{N}_2$  from the INMS data for  $T_b$  egress (from fig. 6 in De La Haye *et al.* 2007a): dashed lines (thermal profiles,  $T_{\text{th}} = 149.0$  K (egress)) are the assumed isothermal fits based on data below the exobase (approx. 1450 km); this shows a change in slope of the density profiles above the nominal exobase.

#### 4. Escape flux: pre-Cassini

Titan has a thick and extended atmosphere, which consists of over 95 per cent  $\text{N}_2$ , approximately 2–3 per cent  $\text{CH}_4$  with some  $\text{H}_2$  and other minor species. Loss of hydrogen was known to occur by thermal escape (Lebonnois *et al.* 2003). Heating effects in the exobase region induced by the ambient plasma ions, pick-up ions, ionospheric outflow and energetic re-impacting neutrals have been estimated by a number of groups. Initial estimates for atmospheric sputtering of nitrogen induced by magnetospheric ions penetrating Titan's atmosphere were large (Lammer & Bauer 1993). Therefore, a three-dimensional DSMC calculation of the atmospheric sputtering (Michael *et al.* 2005a) and a one-dimensional DSMC simulation of the plasma-induced heating were carried out using a model plasma flux consisting of magnetospheric and pick-up ions (e.g. Shematovich *et al.* 2003). However, these simulations led to a very small increase of the exobase temperature (Michael & Johnson 2005) and a modest globally averaged loss rate: approximately  $0.6 \times 10^9$   $\text{amu cm}^{-2} \text{s}^{-1}$  normalized to Titan's surface (Michael *et al.* 2005a).

Initial estimates of the photon- and electron-induced chemistry near the exobase gave significant loss rates (Strobel & Shemansky 1982), but revisions resulted in modest heating and loss rates, e.g. approximately  $0.2 \times 10^9$   $\text{amu cm}^{-2} \text{s}^{-1}$  normalized to Titan's surface as seen in figure 1 (Shematovich *et al.* 2003). Therefore, prior to the arrival of Cassini–Huygens, it was concluded that the present escape rates for carbon and nitrogen species were small. If this was the case, then the observed nitrogen isotope ratios must have evolved in an earlier period when the solar EUV and plasma interactions were more robust (e.g. Lammer *et al.* 2008).

Following the Voyager flybys, it was also assumed that nitrogen escaping from Titan would be the dominant process for supplying Saturn's magnetosphere with heavy ions (Barbosa 1987). However, ions formed near Titan's orbit from the ejected neutrals have a high probability of being lost down Saturn's magnetotail.

Therefore, the dominant source of nitrogen ions to Saturn's magnetosphere appears to be Enceladus (Smith *et al.* 2007, 2008). After reviewing the recent estimates of the escape rate, we compare the various magnetospheric source rates.

## 5. Escape flux: Cassini data

With the many transits of Titan's exobase by Cassini, the escape processes have been re-examined. Data from the Cassini INMS indicate a steeply varying H<sub>2</sub> density profile above the nominal exobase (Waite *et al.* 2005) as seen in figure 2a. This profile is consistent with considerable H<sub>2</sub> escape: a mass flux of H<sub>2</sub> of approximately  $2 \times 10^{10}$  amu cm<sup>-2</sup> s<sup>-1</sup> normalized to the surface of Titan (Cui *et al.* 2008). Assuming that this is a global average, then it is comparable to the pre-Cassini estimates of hydrogen loss (Lebonnois *et al.* 2003). A large H<sub>2</sub> escape flux appears to be roughly consistent with the presence of the extended hydrogen corona imaged by the detection of energetic neutral atoms produced by charge exchange (Garnier *et al.* 2007). Since hydrogen is produced by dissociation of methane and other hydrocarbons, its loss to space implies that atmospheric methane is also lost to the surface, precipitating out as larger hydrocarbons. Using the above hydrogen loss rate, and the atmospheric chemistry model of Wilson & Atreya (2004), methane is lost from the atmosphere by precipitation of hydrocarbons at a rate of approximately  $2 \times 10^{29}$  amu s<sup>-1</sup>. Therefore, even for the largest escape rates discussed below, mass loss to the surface dominates escape to space.

Models of the Cassini INMS data indicate that the heating processes for Titan's atmospheric corona and exobase region are not yet fully understood. De La Haye *et al.* (2007a,b) examined such data for a number of early passes and showed that the structure could be understood if the energy spectra of the molecules in the corona had an enhanced high-energy tail or a non-thermal, hot component. This was suggested by the change in slope near to or above the nominal exobase as indicated in figure 2b for the crossing of the exobase region as Cassini exited Titan's atmosphere during orbit T<sub>b</sub>. However, it is also clear from the five passes through the exobase examined by De La Haye *et al.* (2007a) that the coronal structure varies considerably both spatially and in time.

In order to simulate the densities of N<sub>2</sub> and CH<sub>4</sub> from the nominal exobase (approx. 1450 km) to 2000 km above Titan's surface, De La Haye *et al.* (2007a) found that the energy spectra of the molecules in the hot corona could be well represented by kappa distributions (Vasyliunas 1968; Jurac *et al.* 2002). These are Maxwellian energy distributions that fall off as power laws at higher energies. Such a distribution at the exobase implies that an equilibrium thermal energy distribution well below the exobase developed an energetic tail in the exobase region. For the kappa distributions extracted, the tail decayed with increasing energy much more steeply than the recoil spectra discussed above: powers were approximately 4–20 for cases for which there was a hot nitrogen corona. This steep decay could be an artefact of the narrow range of altitudes modelled, or it could suggest that processes other than the production of hot recoils are responsible for the coronal structure. More importantly, for four of the five exobase crossings examined, De La Haye *et al.* (2007a) could not account for the measured corona structure by assuming that the tail of the distribution was only populated by known photon- and electron-induced chemical processes or by the

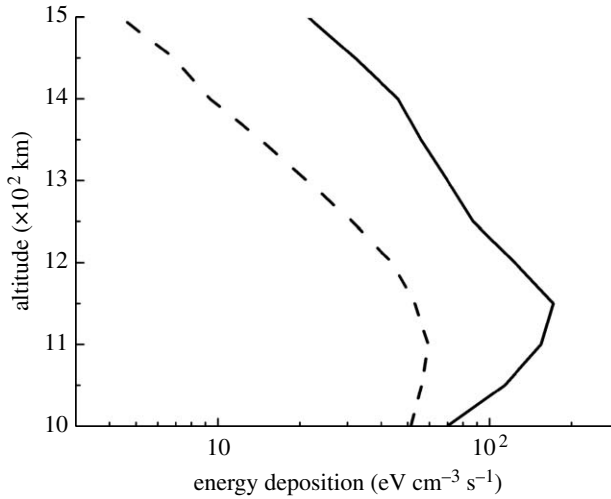


Figure 3. Comparison of heating rates in  $\text{eV cm}^{-3} \text{s}^{-1}$  versus radial distance from Titan's surface: (dashed line) the globally averaged solar EUV/UV at medium solar conditions, net heating with 25% efficiency and HCN cooling (approx. 12% of total near exobase; Strobel 2008); (solid line) the model of the incident plasma used in Michael & Johnson (2005) based on a globally averaged flux of about  $5 \times 10^9 \text{ eV cm}^{-2} \text{ s}^{-1}$  normalized to the exobase surface. No correction for heating efficiency was made, as energy is directly deposited in molecular motion. A comparable cooling due to HCN emission would include an approximately 12% reduction (a globally averaged flux of approx.  $10^9 \text{ eV cm}^{-2} \text{ s}^{-1}$  is a rough lower bound based on recent models and CAPS data, as discussed in the text).

published models of the plasma-induced sputtering rate. That is, additional energy was needed due to either energy transport from below or larger energy deposition rates in the exobase region.

Using best fits to the neutral densities obtained from models of exobase energy distributions, De La Haye *et al.* (2007a) extracted estimates of the energy deposition rate that would be required to produce the local corona structure. This energy could be delivered by exothermic chemistry, by interaction with the plasma or by transport processes. The heating rate required was found to vary from a crossing of the exobase in which no hot corona was identified, hence no hot particle production in the exobase region was required, to relatively large, possibly unrealistic, energy deposition rates in the exobase region. Heating rates were extracted using the best kappa energy distributions and the analytic model described above with  $x=0$ . The average heating rate for the five crossings examined was approximately  $70\text{--}140 \text{ eV cm}^{-3} \text{ s}^{-1}$  depending on the model energy distribution used. As indicated above, such energy deposition rates near the nominal exobase are much larger than the estimates for the photo-induced heating minus cooling at that altitude (approx.  $8 \text{ eV cm}^{-3} \text{ s}^{-1}$ ; Strobel 2008) and much larger than the earlier estimates of the plasma-induced heating rate (approx.  $15 \text{ eV cm}^{-3} \text{ s}^{-1}$ , Lammer *et al.* 1998; approx.  $20 \text{ eV cm}^{-3} \text{ s}^{-1}$ , Michael & Johnson 2005; e.g. figure 3). They concluded that plasma-induced heating associated with the magnetosphere-ionosphere interaction was likely to be more important than the pre-Cassini estimates. This assumption appears to this author to be consistent with the observation by the Cassini Plasma Spectrometer

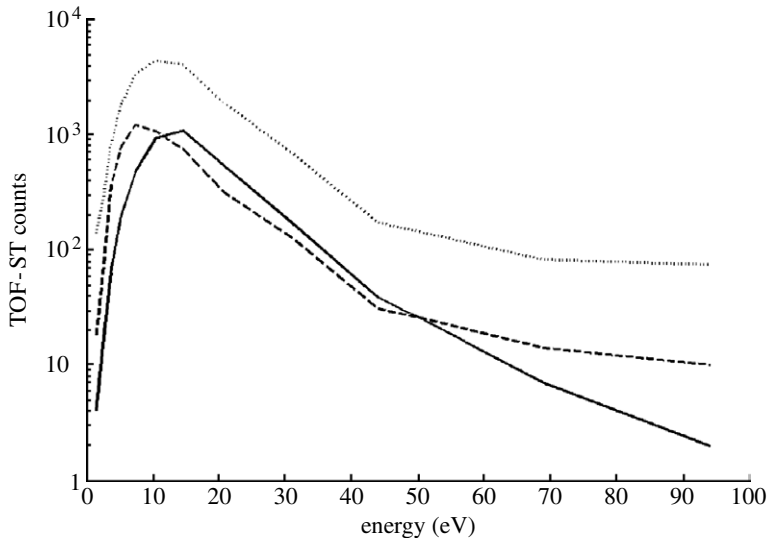


Figure 4. Energy distribution for ions above Titan's exobase (approx. 1680 km) on the egress portion of Cassini orbit  $T_a$  obtained from CAPS time-of-flight, straight-through (TOF-ST) data: results are given for the two principal heavy-ion mass peaks (Michael *et al.* 2005b). Model plasma ion energy spectra used in simulations of atmospheric sputtering (e.g. Shematovich *et al.* 2003) and in obtaining the solid curve in figure 3 had a cut-off at approximately 50 eV. Dashed line,  $M$  12–16; solid line,  $M$  28–29; dotted line, total.

(CAPS) instrument of a flux of low-energy ions in the corona near the exobase (e.g. figure 4). These low-energy ions, which couple more efficiently to the neutrals, were absent from the hybrid simulations that were used to obtain the plasma heating rate in figure 3. They are probably associated with pick-up close to the exobase and/or ionospheric outflow, i.e. ions scavenged from the ionosphere (Wahlund *et al.* 2005; Hartle *et al.* 2006a,b; Ma *et al.* 2006; Sillanpaa *et al.* 2006). Such ions flowing through the corona can efficiently heat the atmosphere in the exobase region due to long-range ion–neutral interactions. Although the absolute fluxes in figure 4 are not yet available, the peak count rate measured is more than an order of magnitude larger than the peak ion count rate in the ambient plasma.

Since the kappa energy spectra extracted from the fits to the INMS data had a steeply decaying tail, the average escape rates for  $\text{CH}_4$  and  $\text{N}_2$  were very small. However, for that range of altitudes for which  $\text{CH}_4$  and  $\text{N}_2$  density information was available (up to approx. 2000 km above the surface), these spectra were well tested for energies only up to about a seventh of the local escape energy. Assuming that the heating rates extracted are due to a production of recoils in the thermosphere, the energy deposition rates found by De La Haye *et al.* (2007a) were scaled to the plasma-induced sputtering rate obtained by Michael *et al.* (2005a). This is valid as long as the primary recoils have energies larger than the escape energy. The average escape flux found in this manner for the five exobase crossings is approximately  $0.3 \times 10^{10} \text{ amu cm}^{-2} \text{ s}^{-1}$  measured with respect to Titan's surface, with nitrogen mass loss about twice that of methane. If correct, this is much larger than the escape rates obtained from the pre-Cassini

simulations. They also obtain what they feel is a rough upper bound by assuming that the tail of the energy spectrum is determined using the recoil energy distribution described earlier. This is the analytic model of the hot corona in De La Haye *et al.* (2007a; e.g. table 5). Averaging these escape rates for the five passes and summing the N<sub>2</sub> and CH<sub>4</sub> contributions gives an average mass flux out equal to approximately  $5 \times 10^{10}$  amu cm<sup>-2</sup> s<sup>-1</sup> normalized to Titan's surface. Assuming that this applies globally, their averaged upper bound to the loss rate is approximately  $4 \times 10^{28}$  amu s<sup>-1</sup> presumed due to plasma-induced heating.

Examining Cassini data below the exobase using continuum models, Strobel (2008) and Yelle *et al.* (2008) separately concluded that, in addition to H<sub>2</sub> loss, escape of a heavy species was occurring. However, their suggested mechanism for escape was very different from that described above. Strobel (2008) modelled the density and temperature profile using an approximate fluid dynamic model that included thermal conductivity and solar heating. Three cases were examined: a lower boundary that allowed a heat flux, and two different net heating/cooling rates with peaks occurring well below the exobase (e.g. figure 3). The observed altitude dependence of the mass density and the Huygens Atmospheric Structure Instrument (HASI) temperature profile (Fulchignoni *et al.* 2005) could be well represented by having an upward mass flux of approximately  $5 \times 10^{10}$  amu cm<sup>-2</sup> s<sup>-1</sup> measured from Titan's surface. Continuing the fluid model above the exobase, Strobel found that thermal conduction could drive escape. Although calculated to be consistent with the mass density profile, the escape flux was presumed to be dominated by the lighter species, CH<sub>4</sub> and H<sub>2</sub>, due to diffusive separation.

Yelle *et al.* (2008) noted that the changing atmospheric composition with altitude in the thermosphere (e.g. figure 2a,b) is indicative of diffusion of CH<sub>4</sub> through the background N<sub>2</sub>. They derived eddy diffusivity from the density profile for <sup>40</sup>Ar and then solved the coupled diffusion equations using eddy and molecular diffusion, allowing for the possibility of upward flow. Modelling up to the nominal exobase, they found that the combined CH<sub>4</sub> and N<sub>2</sub> profiles could be described if CH<sub>4</sub> flows upwards at a rate of approximately  $4\text{--}5 \times 10^{10}$  amu cm<sup>-2</sup> s<sup>-1</sup>. They then presumed that this was a measure of the loss to space, rather than the loss of methane by any other process. This mass flux is remarkably close to that found by Strobel (2008). It is also close to the average upper limit for escape in De La Haye *et al.* (2007a). Therefore, ignoring the very lowest escape estimates in De La Haye *et al.*, the three models of the Cassini data suggest that Titan could be experiencing an average escape flux of the order of approximately  $0.3\text{--}5 \times 10^{10}$  amu cm<sup>-2</sup> s<sup>-1</sup> in heavy molecules. Such rates are much larger than the pre-Cassini estimates.

## 6. Comparison of estimates for escape

Although all three papers suggest that the heavy-molecule loss rate may be larger than anticipated, there are considerable differences between the analyses in Strobel (2008) and Yelle *et al.* (2008) and that in De La Haye *et al.* (2007a). The former are continuum models that are solved up to the exobase. In these models, it is assumed that solar heating of the atmosphere well below the exobase is transported upwards by thermal conduction that can operate above the

exobase to power the escape. De La Haye *et al.* (2007a), on the other hand, modelled a few passes and hypothesized that escape was powered by the molecular physics occurring in the thermosphere and corona, and that the background temperature produced by solar heating is nearly isothermal, with the energy deposition roughly compensating for the adiabatic cooling by escape.

Although different conceptually, these results could be made to be consistent. That is, if atmosphere is being removed at the top by a process similar to that in De La Haye *et al.*, then, in a one-dimensional model, there must be an average upward flow replacing the material removed. Vice versa, the presence of an upward flow below the exobase found in the continuum models could be consistent with the heavy species being removed at the top by any number of processes: ionospheric outflow, pick-up ion loss, atmospheric sputtering, radiation chemistry and precipitation, viscous momentum transport from H<sub>2</sub>, transport to another region of the atmosphere or any combination of these processes.

However, the very different mechanisms for powering escape, as described in these papers, deserve comment. In the fluid models, after concluding that there is a net upward flux in the thermosphere below the exobase, Strobel (2008) and Yelle *et al.* (2008) assumed that the production of hot recoils or other atmospheric removal processes in the vicinity of the exobase are not required. Rather, they propose that thermal conduction from below produces a non-thermal tail in the exobase region and continues to act above the exobase to accelerate a fraction of the coronal particles to escape energies. Such a model could be consistent with the steep power laws in the kappa distributions derived below 2000 km. But those spectra led to very small escape fluxes. In order to obtain the larger escapes rates, De La Haye *et al.* assumed that molecular processes act to produce hot recoils throughout the region of the thermosphere defined by the escape depths in figure 1.

It may also be noteworthy that the coronal enhancements for the five individual passes analysed in De La Haye *et al.* (2007a,b) do not appear to correlate with solar heating. For example, there appears to be no enhanced corona for T<sub>5</sub> ingress, although the atmosphere below the exobase is exposed to the solar flux. However, on the egress portion of this orbit there appears to be an enhanced corona above an atmosphere that has not been exposed to the Sun for a large fraction of a Titan night (8 days). Similarly, the most robust corona, which De La Haye *et al.* (2007a) assumed to be caused by the largest exobase heating effect, was seen on the exobase crossing for T<sub>b</sub> egress (figure 2b), a crossing point that is above a region of the atmosphere not exposed to the Sun. Such observations, of course, do not eliminate solar heating and thermal conduction as the driving mechanism, since time lags and horizontal transport (Mueller-Wodarg *et al.* 2008) have been shown to be important and need to be described. In addition, since simulations of the spatial variations in the plasma flow through the exobase region (e.g. Ledvina *et al.* 2005; Sillanpaa *et al.* 2007) indicate that the plasma-induced heating has a very different morphology than solar heating, both processes eventually need to be included in a three-dimensional model.

The analysis in De La Haye *et al.* (2007a) used a description of the hot particles produced below the exobase and tracked them ballistically (Liouville's theorem) above the nominal exobase assuming no subsequent collisions. By contrast, the fluid models conclude that thermal conduction occurs above the exobase with a sufficient collision rate to produce a significant escape flux. There are, of course, collisions above the nominal exobase (Schunk & Nagy 2000). However, the enhancement

required in the energetic tail is significant. Using a temperature of 150 K, corresponding to a  $\text{CH}_4$  thermal speed of approximately  $0.45 \text{ km s}^{-1}$ , a mass flow speed of approximately  $0.013 \text{ km s}^{-1}$  and a density of approximately  $2 \times 10^6 \text{ CH}_4 \text{ cm}^{-3}$  at the exobase corresponding to  $10^{10} \text{ amu cm}^{-2} \text{ s}^{-1}$ , the fraction of the upwardly moving  $\text{CH}_4$  with escape energies at the nominal exobase density is  $\leq 10^{-11}$ . In order to account for the proposed escape flux, this fraction has to increase to approximately 0.5 per cent of the upwardly moving neutrals having speeds of approximately  $2.1 \text{ km s}^{-1}$ , the escape speed. This does not require a large amount of energy. However, it does require a large number of collisions in the tail of the distribution in a region in which collisions, although occurring, are infrequent.

Although the density profile below the exobase can be reasonably well described by an isothermal atmosphere, modulated by gravity waves (Waite *et al.* 2005; Mueller-Wodarg *et al.* 2006), the continuum models predict temperature profiles in which  $T$  decreases as a function of altitude in the thermosphere consistent with cooling associated with upward heat flow and which equally well fit the average density profile measured by INMS. A recent two-dimensional model of the Northern Hemisphere, the region primarily sampled by Cassini (Mueller-Wodarg *et al.* 2008), also shows a slightly decreasing  $T$  profile everywhere above approximately 1400 km, but the uncertainties in these temperatures are large and increase at increasing altitudes. Therefore, associating the upward flows with global transport cannot be ruled out. De La Haye *et al.* (2007a), on the other hand, hypothesize that there is an additional, and spatially variable, source of hot recoils in the thermosphere and corona near the exobase producing the spatially variable coronal structure observed. The source of these recoils has not yet been identified. Possible processes are reviewed below.

## 7. Coronal heating and loss processes

In addition to thermal conduction and gravity waves from below, there are a number of processes that act on the neutrals in Titan's corona and exobase region. The upward flow of hydrogen molecules having thermal speeds much greater than that for the heavy molecules (approx.  $1.2 \text{ km s}^{-1}$  at 150 K) can, in principle, transfer momentum to the heavy molecules (e.g. Chamberlain & Hunten 1987). Cui *et al.* (2008) model the viscous energy loss to the heavy background molecules as part of their 13 moment approximation to the Boltzmann equation (Schunk & Nagy 2000). In this model, viscosity and heat conduction can, in principle, produce a Maxwellian with an enhanced tail, conceptually similar to the kappa distribution for the heavy species (De La Haye *et al.* 2007a). But the viscous heating rate in their fig. 7 (approx.  $2 \text{ eV cm}^{-3} \text{ s}^{-1}$ ) falls short of that required to drive the outflow of the heavy molecules. In fact, the modelling in Cui *et al.* (2008) requires that the  $\text{H}_2$  molecules draw energy from the background gas, enhancing the tail of the  $\text{H}_2$  velocity distribution function.

The production of hot recoils in the thermosphere by the solar EUV and UV photons could have been underestimated in De La Haye *et al.* (2007a,b). But in the absence of new exothermic processes, the present estimates for recoil production are not sufficient to drive the largest  $\text{CH}_4$  escape flux suggested. Magnetohydrodynamic (MHD) and hybrid simulations show that the slowed and deflected ambient

plasma, and the locally produced pick-up ions, can have access to neutrals in the corona and the upper thermosphere. Atmospheric loss occurs by momentum transfer collisions and charge exchange with the incident ions, producing neutrals with energies greater than the escape energy. Ionization of neutrals by charge exchange, electron impact and photons followed by pick-up ion formation can also lead to atmospheric loss (Ma *et al.* 2006; Sillanpaa *et al.* 2006). Since the fields penetrate below the exobase, ionospheric outflow also occurs (Wahlund *et al.* 2005; Hartle *et al.* 2006a,b; Coates *et al.* 2007), as seen at Io (e.g. Wilson *et al.* 2002) and Venus (e.g. Terada *et al.* 2004). The ionospheric outflow, pick-up ions and the slowed and deflected ambient ions, as well as the energetic neutrals produced by charge exchange, collisionally deposit energy in the corona, causing atmospheric sputtering. These plasma heating processes can be important at altitudes well above the exobase, as the ion–neutral momentum transfer cross-section is an order of magnitude larger than the neutral–neutral cross-section.

The escape rate derived in Strobel (2008) requires the delivery of approximately  $6 \times 10^8 \text{ eV cm}^{-2} \text{ s}^{-1}$ . The average energy deposition rate extracted by De La Haye *et al.* (2007a;  $70\text{--}140 \text{ eV cm}^{-3} \text{ s}^{-1}$ ), deposited over a scale height (approx. 60 km), suggests a similar energy flux (approx.  $4\text{--}8 \times 10^8 \text{ eV cm}^{-2} \text{ s}^{-1}$ ), which they presumed to be deposited in hot recoil production. The energy flux available in the ambient plasma and fields is larger than this,  $10^{10} \text{ eV cm}^{-2} \text{ s}^{-1}$  (e.g. Johnson 2004). This flux ignores any enhancement in the effective area of interaction due to the expanded corona or the gyroradii of the heavy ions (Hartle *et al.* 2006a,b). Although this indicates that sufficient energy is, in principle, available from the magnetosphere–atmosphere interaction, a significant fraction will be carried by the energetic plasma and deposited at depth. Therefore, molecular level modelling in the interaction region combined with Cassini data will be required to determine if the plasma-induced escape rates are indeed much larger than the earlier estimates. For instance, the energy flux used to obtain the exobase heating rate given in figure 3 is approximately  $5 \times 10^9 \text{ eV cm}^{-2} \text{ s}^{-1}$  (Michael & Johnson 2005; Michael *et al.* 2005a). Although this is larger than that required by De La Haye *et al.*, it is seen to be deposited mostly a few scale heights below the exobase. This resulted in a temperature profile that slightly increases with increasing altitude but still produces atmospheric loss rates well below the recent estimates. Therefore, the details of the collisional coupling of the ions to the neutrals are critical. That is, if the incident plasma had a similar energy flux, but an energy spectrum such as that in figure 4, the energy would be deposited in a much narrower region about the exobase, increasing the escape rate.

Using CAPS data Hartle *et al.* (2006a,b) estimated that approximately  $0.9 \times 10^{24} \text{ O}^+ \text{ s}^{-1}$  impact Titan's atmosphere and corona. Since these ions have mean flow energies in the keV range and comparable thermal energies, they contribute a significant fraction of the energy flux used to obtain the plasma-induced heating rate in figure 3. Consistent with this, Sillanpaa *et al.* (2007) find that approximately  $10^{24} \text{ O}^+ \text{ s}^{-1}$  are lost to interactions with Titan, depositing a globally averaged energy flux of approximately  $10^9 \text{ eV cm}^{-2} \text{ s}^{-1}$  normalized to the exobase surface. Estimates to date of the rate of energy deposition into recoils by the incoming ions using hybrid and MHD models (Brecht *et al.* 2000; Ledvina *et al.* 2005; Sillanpaa *et al.* 2007; Tseng *et al.* 2008) are below that required by De La Haye *et al.* (2007a). In such simulations, the ion energy deposition rate

into the atmosphere is affected by the fields penetrating the exobase region. Therefore, modelling the ion and energetic neutral flow through the exobase region and their collisional coupling to the background neutrals is critical. For instance, ions and energetic neutrals penetrating the edge of the atmosphere (Michael *et al.* 2005a), pick-up ions formed close to the exobase, and ions outflowing from the ionosphere can cross the exobase from below. This process, referred to as forward sputtering, can considerably enhance the sputtering efficiency (Johnson 1990, 1994). Based on CAPS data (e.g. figure 4) and data from other instruments (e.g. Wahlund *et al.* 2005), there is a flux of low-energy ions flowing through the corona that has not yet been incorporated into the atmospheric sputtering simulations. There is also a flux of very energetic ions ( $\gg 10$  keV; Ledvina *et al.* 2005), but these ions deposit their energy at depth (e.g. Luna *et al.* 2003; Cravens *et al.* 2008) and do not affect escape.

If atmospheric sputtering is the dominant process driving escape, which is not at all clear, it is the low-energy heavy pick-up and ionospheric ions that need to be included in new simulations of Titan's exobase region. Fortunately, more detailed models of the plasma flow through the exobase region, constrained by Cassini plasma data, are now becoming available.

## 8. Summary

Based on data from Cassini for many passes through Titan's upper atmosphere, we are rapidly improving our knowledge of atmospheric escape as well as our knowledge of the interaction of Saturn's magnetosphere with Titan's atmosphere. In order to describe the evolution of this unique atmosphere, it is exciting that molecular level modelling of the present escape mechanisms, constrained by Cassini data, is now possible. Therefore, the differences in the loss mechanisms proposed will be resolved by detailed simulations of the transition region in Titan's atmosphere.

Although the hydrogen loss rate (approx.  $2 \times 10^{28}$  amu s<sup>-1</sup>) is similar to the pre-Cassini estimate (Cui *et al.* 2008), considerable enhancements in the loss rate of heavy species have been suggested: approximately  $0.3\text{--}5 \times 10^{28}$  amu s<sup>-1</sup>. If the largest loss rates for the heavy species persisted for *ca* 4 Gyr, the net mass loss would be of the order of the present atmospheric mass. In addition, if such loss rates were primarily in the form of CH<sub>4</sub>, then the present CH<sub>4</sub> inventory would be lost in less than 10<sup>8</sup> years. Although this rate is about an order of magnitude smaller than methane loss by precipitation of hydrocarbons, it can have a significant affect on model descriptions of atmospheric evolution (e.g. Lammer *et al.* 2008). For this reason accurately understanding the mechanisms driving escape (e.g. Johnson *et al.* 2008, submitted) is critical to our understanding of the evolution of Titan's atmosphere.

The escape rate of heavy species estimated in De La Haye *et al.* (2007a) had a wide range of values because the density data only covered a limited range of altitudes above the nominal exobase. If the kappa energy distributions they extracted are correct, then heavy-molecule escape is small, consistent with pre-Cassini estimates. Their preferred escape rate, obtained by scaling the recoil production to earlier simulations, showed a considerable enhancement in the heavy-molecule escape rate (approx.  $0.3 \times 10^{28}$  amu s<sup>-1</sup>), but much smaller than

Table 1. Neutral sources for Saturn's magnetosphere.

source	rate ( $10^{29}$ amu s $^{-1}$ )	composition <sup>a</sup>
rings (Johnson <i>et al.</i> 2006 <i>b</i> )	~6	O <sub>2</sub> , H <sub>2</sub>
Enceladus (Johnson <i>et al.</i> 2006 <i>a</i> )	~2	H <sub>2</sub> O (~4% C or N species)
Titan (De La Haye <i>et al.</i> 2007 <i>a</i> (N <sub>2</sub> , CH <sub>4</sub> ); Cui <i>et al.</i> 2008 (H <sub>2</sub> ); Strobel 2008 (CH <sub>4</sub> , H <sub>2</sub> ); Yelle <i>et al.</i> 2008 (CH <sub>4</sub> ))	0.2–0.5	(N <sub>2</sub> ), CH <sub>4</sub> , H <sub>2</sub>

<sup>a</sup>Molecular dissociation products would also be present for all of these species.

that suggested by Strobel (2008) and Yelle *et al.* (2008). Their rough average upper limit for the mass escape rate was obtained using a model recoil spectrum. If the extracted rate is correct, then a one-dimensional analysis of the density data below the exobase would result in an upward flow such as that found in the other models. In that case, the three mass loss rates would be consistent, although the mechanisms proposed are very different.

For this reason, it is critical to obtain good estimates of the amount and spatial morphology of the plasma-induced heating, the process that was assumed to be driving escape in De La Haye *et al.* Although, the plasma energy deposition rate in the exobase regions is at least as large as the average EUV heating rate, a larger rate or more efficient coupling to the neutrals would be required to obtain the suggested escape rates. If the largest estimates for heavy-molecule escape are viable, but the plasma heating is inadequate, then one of the following must be true: another non-thermal process must be active; the upward flow is indicative of transport to another region of the atmosphere; or heat from below acts to drive escape as proposed by Yelle *et al.* and Strobel. Since a new model for thermal escape has also been proposed for hydrogen loss (Cui *et al.* 2008), molecular level tests of these results are needed. Therefore, stochastic simulations of the gas in the exobase region are critical if we are to obtain an understanding of molecular transport and escape at Titan.

Loss of atmosphere from Titan is not only of evolutionary interest, but also of interest as a source of material for Saturn's magnetosphere. Therefore, the composition of the ambient plasma near Titan's orbit can be used to test the atmospheric loss rate. Prior to the arrival of Cassini, Titan was assumed to be an important, and probably dominant, source of nitrogen for the magnetosphere. Not only is this not the case (e.g. Smith *et al.* 2005, 2007), Titan is not the dominant source of material for Saturn's magnetosphere even for the largest proposed loss rates as seen in table 1. However, if the largest methane source rate (approx.  $4\text{--}5 \times 10^{28}$  amu s $^{-1}$ ; Strobel 2008; Yelle *et al.* 2008) is correct, then Titan is the dominant source of carbon for the magnetosphere.

Since neutrals ejected from Titan orbit Saturn until they are ionized, they can be detected in the ambient plasma. Detection is possible not only close to Titan's orbit, but over a broad region of Saturn's magnetosphere (Smith *et al.* 2004). Although the neutrals converted to ions close to Titan, or in its wake, are rapidly lost down the magnetotail, a background plasma is present in the vicinity of Titan's orbit. Outward diffusion of ions produced closer to Saturn can contribute to this plasma, but such ions are also lost down the magnetotail prior to crossing

Titan's orbit. For this reason the measured phase-space distributions of detected ions indicate that the ambient plasma near Titan's orbit is dominated by neutrals ionized in the outer magnetosphere (Szego *et al.* 2005). Therefore, for the largest methane loss rates proposed, carbon-containing ions should dominate oxygen ions near Titan's orbit. This is the case since the latter must be scattered to the outer magnetosphere from the Enceladus and OH tori (Johnson *et al.* 2006a) or from the ring atmosphere (Johnson *et al.* 2006b). However, the plasma upstream from Titan has been shown to contain a substantial fraction of  $O^+$  (Hartle *et al.* 2006b). A ratio of oxygen to carbon species on Cassini's first orbit of Saturn was estimated to be approximately 1.5 (Crary *et al.* submitted). Scaling the suggested loss rates to earlier models of the neutral densities from all sources (e.g. Smith *et al.* 2004, 2005, 2007; Johnson *et al.* 2006a,b), this fraction is inconsistent with the highest methane source rates suggested. To settle the present carbon escape rate using ion density measurements in the magnetosphere will require a good model of the oxygen and carbon neutral densities and ionization rates near Titan's orbit. In addition, the carbon and oxygen fractions in the ambient plasma will have to be measured for a variety of plasma conditions. However, it is exciting that the concepts for escape from Titan's atmosphere are being re-examined based on recent Cassini data. This is especially so since understanding the present atmospheric escape processes is a precondition for understanding the origin and evolution of Titan's atmosphere.

Support is acknowledged from the Royal Society of London for participation in the Titan Workshop, from NASA's Planetary Atmospheres Program, from the Cassini Program via SwRI and from NASA's Cassini Data Analysis Program.

## References

- Barbosa, D. D. 1987 Titan's atomic nitrogen torus: inferred properties and consequences for the Saturnian aurora. *Icarus* **72**, 53–61. (doi:10.1016/0019-1035(87)90118-7)
- Brecht, S. H., Luhmann, J. G. & Larson, D. J. 2000 Simulation of the Saturnian magnetospheric interaction with Titan. *J. Geophys. Res.* **105**, 13 119–13 130. (doi:10.1029/1999JA900490)
- Chamberlain, J. W. & Hunten, D. 1987 *Theory of planetary atmosphere*. New York, NY: Academic Press.
- Cipriani, F., Leblanc, F. & Berthelier, J. J. 2007 Martian corona: nonthermal sources of hot heavy species. *J. Geophys. Res.* **112**, E07001. (doi:10.1029/2006JE002818)
- Coates, A. J., Crary, F. J., Young, D. T., Szego, K., Arridge, C. S., Bebesi, Z., Sittler Jr, E. C., Hartle, R. E. & Hill, T. W. 2007 Ionospheric electrons in Titan's tail: plasma structure during the Cassini T9 encounter. *Geophys. Res. Lett.* **34**, L24S05. (doi:10.1029/2007GL030919)
- Crary, F. J. *et al.* Submitted. Dynamics and composition of plasma at Titan. In *Titan after Cassini-Huygens* (ed. R. Brown *et al.*). Tucson, AZ: University of Arizona Press.
- Cravens, T. E., Robertson, I. P., Ledvina, S. A., Mitchell, D., Krimigis, S. M. & Waite, J. H. 2008 Energetic ion precipitation at Titan. *Geophys. Res. Lett.* **35**, L03103. (doi:10.1029/2007GL032451)
- Cui, J., Yelle, R. V. & Volk, K. 2008 Distribution and escape of molecular hydrogen in Titan's thermosphere and exosphere. *J. Geophys. Res.* **113**, E10004. (doi:10.1029/2007JE003032)
- De La Haye, V. *et al.* 2007a Cassini Ion and Neutral Mass Spectrometer data in Titan's upper atmosphere and exosphere: observation of a suprathermal corona. *J. Geophys. Res.* **112**, A07309. (doi:10.1029/2006JA012222)
- De La Haye, V., Waite Jr, J. H., Cravens, T. E., Nagy, A. F., Yelle, R. V., Johnson, R. E., Lebonnois, S. & Robertson, I. P. 2007b Titan's corona: the contribution of exothermic chemistry. *Icarus* **191**, 236–250. (doi:10.1016/j.icarus.2007.04.031)

- Fulchignoni, M. *et al.* 2005 Titan's physical characteristics measured by the Huygens Atmospheric Structure Instrument (HASI). *Nature* **438**, 785–791. (doi:10.1038/nature04314)
- Garnier, P. *et al.* 2007 The exosphere of Titan and its interaction with the Kronian magnetosphere: MIMI observations and modeling. *Planet. Space Sci.* **55**, 165–173. (doi:10.1016/j.pss.2006.07.006)
- Hartle, R. E. *et al.* 2006a Preliminary interpretation of Titan plasma interaction as observed by the Cassini Plasma Spectrometer: comparisons with Voyager 1. *Geophys. Res. Lett.* **33**, L08201. (doi:10.1029/2005GL024817)
- Hartle, R. E. *et al.* 2006b Initial interpretation of Titan plasma interaction as observed by the Cassini Plasma Spectrometer: comparisons with Voyager 1. *Planet. Space Sci.* **54**, 1211–1224. (doi:10.1016/j.pss.2006.05.029)
- Hirschfelder, J. O., Curtiss, C. F. & Bird, R. B. 1964 *Molecular theory of gases and liquids*. New York, NY: Wiley. (2nd corrected printing)
- Johnson, R. E. 1990 *Energetic charged-particle interactions with atmospheres and surfaces*. Berlin, Germany: Springer.
- Johnson, R. E. 1994 Plasma-induced sputtering of an atmosphere. *Space Sci. Rev.* **69**, 215–253. (doi:10.1007/BF02101697)
- Johnson, R. E. 2004 The magnetospheric-plasma-driven evolution of satellite atmospheres. *Astrophys. J.* **609**, L99–L102. (doi:10.1086/422912)
- Johnson, R. E. & Luhmann, J. G. 1998 Sputtering contribution to the atmospheric corona on Mars. *J. Geophys. Res.* **103**, 3649–3653. (doi:10.1029/97JE03266)
- Johnson, R. E., Schnellenger, D. & Wong, M. C. 2000 The sputtering of an oxygen thermosphere by energetic O<sup>+</sup>. *J. Geophys. Res.* **105**, 1659–1670. (doi:10.1029/1999JE001058)
- Johnson, R. E., Smith, H. T., Tucker, O. J., Liu, M. & Tokar, R. 2006a The Enceladus and OH tori at Saturn. *Astrophys. J. Lett.* **644**, L137–L139. (doi:10.1086/505750)
- Johnson, R. E. *et al.* 2006b Production, ionization and redistribution of O<sub>2</sub> in Saturn's ring atmosphere. *Icarus* **180**, 393–402. (doi:10.1016/j.icarus.2005.08.021)
- Johnson, R. E., Combi, M. R., Fox, J. L., Ip, W.-H., Leblanc, F., McGrath, M. A., Shematovich, V. I., Strobel, D. F. & Waite Jr, J. H. 2008 Exospheres and atmospheric escape. *Space Sci. Rev.* **139**, 355–397. (doi:10.1007/s11214-008-9415-3)
- Johnson, R. E., Tucker, O. J., Michael, M., Sittler, E. C., Waite, J. H. & Young, D. A. Submitted. Mass loss processes at Titan. In *Titan after Cassini–Huygens* (ed. R. Brown *et al.*). Tucson, AZ: University of Arizona Press.
- Jurac, S., McGrath, M. A., Johnson, R. E., Richardson, J. D., Vasyliunas, V. M. & Eviatar, A. 2002 Saturn: search for a missing water source. *Geophys. Res. Lett.* **29**, 2172. (doi:10.1029/2002GL015855)
- Lammer, H. & Bauer, S. J. 1993 Atmospheric mass loss from Titan by sputtering. *Planet. Space Sci.* **41**, 657–663. (doi:10.1016/0032-0633(93)90049-8)
- Lammer, H., Stumptner, W. & Bauer, S. J. 1998 Dynamic escape of H from Titan as a consequence of sputtering induced heating. *Planet. Space Sci.* **46**, 1207–1213. (doi:10.1016/S0032-0633(98)00050-6)
- Lammer, H., Kasting, J. F., Chassefière, E., Johnson, R. E., Kulikov, Y. N. & Tian, F. 2008 Atmospheric escape and evolution of terrestrial planets and satellites. *Space Sci. Rev.* **139**, 399–436. (doi:10.1007/s11214-008-9413-5)
- Lebonnois, S., Bakes, E. L. O. & McKay, C. P. 2003 Atomic and molecular hydrogen budget in Titan's atmosphere. *Icarus* **161**, 474–485. (doi:10.1016/S0019-1035(02)00039-8)
- Ledvina, S. A., Cravens, T. E. & Kecskemety, K. 2005 Ion distributions in Saturn's magnetosphere near Titan. *J. Geophys. Res.* **110**, A06211. (doi:10.1029/2004JA010771)
- Luna, H., Michael, M., Shah, M. B., Johnson, R. E., Latimer, C. J. & McConkey, J. W. 2003 Dissociation of N<sub>2</sub> in capture and ionization collisions with fast H<sup>+</sup> and N<sup>+</sup> ions and modeling of positive ion formation in the Titan atmosphere. *J. Geophys. Res.* **108**, 5033. (doi:10.1029/2002JE001950)

- Ma, Y., Nagy, A. F., Cravens, T. E. I., Sokolov, V., Hansen, K. C., Wahlund, J.-E., Crary, F. J., Coates, A. J. & Dougherty, M. K. 2006 Comparisons between MHD model calculations and observations of Cassini flybys of Titan. *J. Geophys. Res.* **111**, A05207. (doi:10.1029/2005JA011481)
- Michael, M. & Johnson, R. E. 2005 Energy deposition of pickup ions and heating of Titan's atmosphere. *Planet. Space Sci.* **53**, 1510–1514. (doi:10.1016/j.pss.2005.08.001)
- Michael, M., Johnson, R. E., Leblanc, F., Liu, M., Luhmann, J. G. & Shematovich, V. I. 2005a Ejection of nitrogen from Titan's atmosphere by magnetospheric ions and pick-up ions. *Icarus* **175**, 263–267. (doi:10.1016/j.icarus.2004.11.004)
- Michael, M. *et al.* 2005b Atmospheric sputtering and heating. In *Spring 2005 Crete Titan/Cassini-Huygens Meeting, Crete, Greece*.
- Mueller-Wodarg, I. C. F., Yelle, R. V., Borggren, N. & Waite Jr, J. H. 2006 Waves and horizontal structures in Titan's thermosphere. *J. Geophys. Res.* **111**, A12315. (doi:10.1029/2006JA011961)
- Mueller-Wodarg, I. C. F., Yelle, R. V., Cui, J. & Waite Jr, J. H. 2008 Horizontal structures and dynamics of Titan's thermosphere. *J. Geophys. Res.* **113**, E10005. (doi:10.1029/2007JE003033)
- Nagy, A. F. & Cravens, T. E. 1981 Hot oxygen atoms in the upper atmosphere of Venus. *Geophys. Res. Lett.* **8**, 629–632. (doi:10.1029/GL008i006p00629)
- Niemann, H. B. *et al.* 2005 The abundances of constituents of Titan's atmosphere from the GCMS instrument on the Huygens probe. *Nature* **438**, 779–784. (doi:10.1038/nature04122)
- Penz, T., Lammer, H., Kulikov, Yu. N. & Biernat, H. K. 2005 The influence of the solar particle and radiation environment on Titan's atmosphere evolution. *Adv. Space Res.* **36**, 241–250. (doi:10.1016/j.asr.2005.03.043)
- Schunk, R. W. & Nagy, A. F. 2000 In *Ionospheres: physics, plasma physics, and chemistry* (eds A. J. Dressler, J. T. Houghton & M. J. Rycroft). Cambridge Atmospheric and Space Science Series, pp. 104–147. Cambridge, UK: Cambridge University Press.
- Shematovich, V. I., Johnson, R. E., Michael, M. & Luhmann, J. G. 2003 Nitrogen loss from Titan. *J. Geophys. Res.* **108**, 5087. (doi:10.1029/2003JE002094)
- Sigmund, P. 1981 Sputtering by particle bombardment: theoretical concepts. In *Sputtering by particle bombardment* (ed. R. Behrisch), pp. 9–67. Berlin, Germany: Springer.
- Sillanpaa, I., Kallio, E., Janhunen, P., Schmidt, W., Mursula, K., Vilppola, J. & Tanskanen, P. 2006 Hybrid simulation study of ion escape at Titan for different orbital positions. *Adv. Space Res.* **38**, 799–805. (doi:10.1016/j.asr.2006.01.005)
- Sillanpaa, I., Kallio, E., Jarvinen, R. & Janhunen, P. 2007 Oxygen ions at Titan's exobase in a Voyager 1-type interaction from a hybrid simulation. *J. Geophys. Res.* **112**, 2. (doi:10.1029/2007JA012348)
- Smith, H. T., Johnson, R. E. & Shematovich, V. I. 2004 Titan's atomic and molecular nitrogen tori. *Geophys. Res. Lett.* **31**, L16804. (doi:10.1029/2004GL020580)
- Smith, H. T., Shappirio, M., Sittler, E. C., Reisenfeld, D., Johnson, R. E., Baragiola, R. A., Crary, F. J., McComas, D. J. & Young, D. T. 2005 Discovery of nitrogen in Saturn's inner magnetosphere. *Geophys. Res. Lett.* **32**, L14S03. (doi:10.1029/2005GL022654)
- Smith, H. T., Johnson, R. E., Sittler, E. C., Shappirio, M., Tucker, O. J., Burger, M., Crary, F. J., McComas, D. J. & Young, D. T. 2007 Enceladus: the likely dominant nitrogen source in Saturn's magnetosphere. *Icarus* **188**, 356–366. (doi:10.1016/j.icarus.2006.12.007)
- Smith, H. T., Shappirio, M., Johnson, R. E., Reisenfeld, D., Sittler, E. C., Crary, F. J., McComas, D. J. & Young, D. T. 2008 Enceladus: a potential source of ammonia products and molecular nitrogen for Saturn's magnetosphere. *J. Geophys. Res.* **113**, A11206. (doi:10.1029/2008JA013352)
- Strobel, D. F. 2002 Aeronomic systems on planets, moons, and comets. In *Comparative aeronomy in the Solar System* (eds M. Mendillo, A. Nagy & H. Waite). Geophysical Monograph Series, pp. 7–22. Baltimore, MD: American Geophysical Union.
- Strobel, D. F. 2008 Titan's hydrodynamically escaping atmosphere. *Icarus* **193**, 588–594. (doi:10.1016/j.icarus.2007.08.014)
- Strobel, D. F. & Shemansky, D. E. 1982 EUV emissions from Titan's upper atmosphere: Voyager I encounter. *J. Geophys. Res.* **87**, 1361–1368. (doi:10.1029/JA087iA03p01361)

- Szego, K. *et al.* 2005 The global plasma environment of Titan as observed by Cassini Plasma Spectrometer during the first two close encounters with Titan. *Geophys. Res. Lett.* **32**, L20S05. (doi:10.1029/2005GL022646)
- Terada, N., Shinagawa, H. & Machida, S. 2004 Global hybrid model of the solar wind interaction with the Venus ionosphere: ion escape processes. *Adv. Space Res.* **33**, 161–166. (doi:10.1016/j.asr.2003.05.011)
- Tseng, W.-L., Ip, W.-H. & Kopp, A. 2008 Exospheric heating by pickup ions at Titan. *Adv. Space Res.* **42**, 54–60. (doi:10.1016/j.asr.2008.03.009)
- Vasyliunas, V. M. 1968 A survey of low-energy electrons in the evening sector of the magnetosphere with OGO 1 and OGO 3. *J. Geophys. Res.* **73**, 2839–2885. (doi:10.1029/JA073i009p02839)
- Wahlund, J.-E. *et al.* 2005 Cassini measurements of cold plasma in the ionosphere of Titan. *Science* **308**, 982–986. (doi:10.1126/science.1109807)
- Waite Jr, J. H. *et al.* 2005 Ion Neutral Mass Spectrometer results from the first flyby of Titan. *Science* **308**, 982–986. (doi:10.1126/science.1110652)
- Wilson, E. H. & Atreya, S. K. 2004 Current state of modeling the photochemistry of Titan's mutually dependent atmosphere and ionosphere. *J. Geophys. Res.* **109**, E06002. (doi:10.1029/2003JE002181)
- Wilson, J. K., Mendillo, M., Baumgardner, J., Schneider, N. M., Trauger, J. T. & Flynn, B. 2002 The dual sources of Io's sodium clouds. *Icarus* **157**, 476–489. (doi:10.1006/icar.2002.6821)
- Yelle, R. V., Cui, J. & Mueller-Wodarg, I. C. F. 2008 Methane escape from Titan's atmosphere. *J. Geophys. Res.* **113**, E10003. (doi:10.1029/2007JE003031)